Journal of Chromatography, 559 (1991) 3–26
Elsevier Science Publishers B.V., Amsterdam

CHROM. 23 416

Mathematical model describing dispersion in free solution capillary electrophoresis under stacking conditions

ANDERS VINTHER*
Department of Fermentation Physiology, Novo Nordisk, Lagergårdsvej 2, DK-2820 Gentofte (Denmark)
and
HENRIK SØEBERG
Department of Chemical Engineering, Technical University of Denmark, Building 229, DK-2800 Lyngby (Denmark)

ABSTRACT

From experiments a mathematical model is derived that quantitatively describes the dispersion processes in free solution capillary electrophoresis (FSCE) under both stacking and non-stacking conditions. The dispersion is subdivided into an axial, a radial and an introduction term. The last term includes an eventual stacking process, extraneous injection and diffusion during sample introduction. Each of the dispersive terms is derived and discussed. Guidelines for improved peak efficiency during FSCE analysis with stacking conditions are presented.

INTRODUCTION

In the past decade, high-performance capillary electrophoresis (HPCE) [1,2] has evolved as a very promising technique well suited for the analysis of, *e.g.*, proteins and peptides [3–14]. With the emergence of commercially available instrumentation, HPCE is on the brink of becoming a major analytical technique in the biotechnological industries.

One of the attractive features of HPCE is high peak efficiencies due to the so-called electroosmotic flow profile. As a measure of peak efficiency, theoretical plate numbers, N of the order of 10^5–10^6 are obtainable with optimized experimental conditions.

There are, however, several factors that can significantly decrease N. As peak resolution is proportional to $\sqrt{N}$ [8], a knowledge of these dispersion factors is of major importance in the efforts to improve the resolution of closely eluting peaks once a buffer system has been chosen.

General HPCE dispersion theory has been discussed by *e.g.*, Hjertén [15], Foret *et al.* [16] and Terabe *et al.* [17]. In some of the earliest papers concerning HPCE dispersion theory, axial diffusion was assumed to be the dominant dispersive term [18–21]. Using Einstein's equation for axial diffusion [18], this leads to a simple

0021-9673/91/$03.50

expression for N which suggests that high voltages should be applied. High power inductions do, however, cause excessive band broadening due to Joule heating of the liquid in the capillary tube [18–27]. Power is induced uniformly across the capillary cross-sectional area but is only removed at the wall (and at the capillary ends). This leads to a parabolic flow profile as the electroosmotic mobility is a function of the temperature [22]. Dispersion caused by Joule heating can be minimized by using capillaries with a high surface-to-volume ratio and low-conductivity buffers.

Among the other band-broadening factors considered in the present work are radial diffusion, diffusion during sample intake, sample plug length, detector length, chromatographic effects caused by analyte–wall electrostatic interactions [15], sample overload [21,28] and extraneous injection [29]. The last factor refers to sample introduced simply by insertion of the capillary into the sample solution.

Huang *et al.* [30] showed that the physical length of the sample plug introduced is often the most significant dispersion factor. Hence, a very powerful technique in the efforts to achieve optimum peak efficiency is to stack the original introduced sample zone plug.

Sample stacking (concentration of the analyte zone) is the process that occurs when a voltage is applied along a capillary tube containing a sample plug with a lower specific conductivity than that of the surrounding running buffer. As the electric field strength is inversely proportional to the specific conductivity of the liquid, the field strength is higher along the sample plug compared with the running buffer. In this way the electrophoretic velocity, which is proportional to the field strength, increases and the ionic analyte zone is narrowed. This "reversed dispersion" is termed sample stacking.

Based on experimental results and with reference to isotachophoresis theory [31], we have developed a mathematical free solution capillary electrophoresis (FSCE) [4,32] dispersion model. The aim of the model is to describe quantitatively the complex dispersion processes taking place during both stacking and non-stacking FSCE analysis in a simplified way. This approach is different from the previous models based on isotachophoresis [15].

All the experiments were carried out with biosynthetic human growth hormone (B-hGH) as the analyte. B-hGH is a 22 125 relative molecular mass protein consisting of 191 amino acids with an isoelectric point of *ca.* pH 5. Analysis was performed at pH 8.0, where B-hGH is a convenient choice of analyte as it has a suitable net mobility and is repelled from the negatively charged capillary surface.

EXPERIMENTAL

Materials

Tricine {N-[tris(hydroxymethyl)methyl]glycine} and sodium chloride were purchased from Fluka (Buchs, Switzerland) and B-hGH from Novo Nordisk (Gentofte, Denmark). Fused-silica capillaries were obtained from Polymicro Technologies (Phoenix, AZ, USA). Peak areas were integrated on a Shimadzu C-R5A integrator (Kyoto, Japan).

Methods

Analysis was performed on an Applied Biosystems Model 270A analytical

capillary electrophoresis system. The fused-silica capillaries had an I.D. of 50 μm, an O.D. of 192 μm, a total length of 100 cm and a length of 75 cm to the detector (effective length). From the introduction end to the detector the capillaries were surrounded by a thermostated air-bath operated at 27°C. The electroosmotic flow was determined by measuring the retention time of the peak of neutral species.

Two series of experiments were carried out. Samples were introduced by applying a 16.8-kPa vacuum at the detector end of the capillary. The applied potential was changed from 5 to 30 kV in steps of 5 kV. Detection was performed at 200 nm. During the experiments three 10 m*M* tricine running buffers of pH 8.0 containing (a) 0 m*M* NaCl (specific conductivity at 21°C, $\kappa_{21°C} = 0.22$ mS cm^{-1}), (b) 25 m*M* NaCl ($\kappa_{21°C} = 2.75$ mS cm^{-1}) or (c) 50 m*M* NaCl ($\kappa_{21°C} = 4.96$ mS cm^{-1}) were employed. In the stacking runs B-hGH was diluted with distilled water to 0.1 mg ml^{-1} ($\kappa_{21°C} = 0.17$ mS cm^{-1}), whereas under non-stacking conditions B-hGH was diluted to the same concentration with the 10 m*M* tricine (pH 8.0)–25 m*M* NaCl running buffer.

Experimental series 1 was subdivided in two series with (1A) stacking and (1B) non-stacking conditions. Samples were introduced for 3.0 s. The running buffer was 10 m*M* tricine (pH 8.0)–25 m*M* NaCl. The purpose of series 1 was to show the effect of stacking on peak efficiency.

Experimental series 2 was subdivided in three series all having stacking conditions, but differing in the NaCl concentration in the 10 m*M* tricine running buffer (pH 8.0): (2A) 0, (2B) 25 and (2C) 50 m*M* NaCl. The sample was B-hGH diluted with distilled water to 0.1 mg ml^{-1} and introduced for 1.0 s. The purpose of series 2 was to show the effect of stacking power (defined as the difference between the sample zone and running buffer field strength, ΔE) on peak efficiency.

THEORY

Fig. 1 depicts the number of theoretical plates, N, *vs.* the applied potential, U, in experimental series 1. B-hGH was diluted either in distilled water (1A, stacking, $\kappa_B > \kappa_S$) or in the running buffer (1B, no stacking, $\kappa_B = \kappa_S$). N was calculated based on experimentally obtained results as

$$N = 5.54\left(\frac{t_R}{w_{\frac{1}{2}}}\right)^2 \tag{1}$$

where t_R is the analyte retention time and $w_{\frac{1}{2}}$ is the peak width at half-height (a measure of dispersion).

The highest N values were obtained at low applied potentials (long analysis time), which means that axial diffusion is not the dominant dispersive factor in these experiments [18–20]. Further, it was concluded that the trend of decreasing N at increasing U was not caused by band broadening due to excessive Joule heating [22].

What puzzled us most in Fig. 1, however, was the greatly improved peak efficiencies at low U when non-stacking conditions were changed for stacking conditions. This is clearly demonstrated in Fig. 2, where the experimentally obtained 5-kV stacking electropherogram is shown below on the corresponding 5-kV non-stacking electropherogram. In an attempt to describe and explain these experimental results, in the following a theoretical approach to the dispersion process is presented.

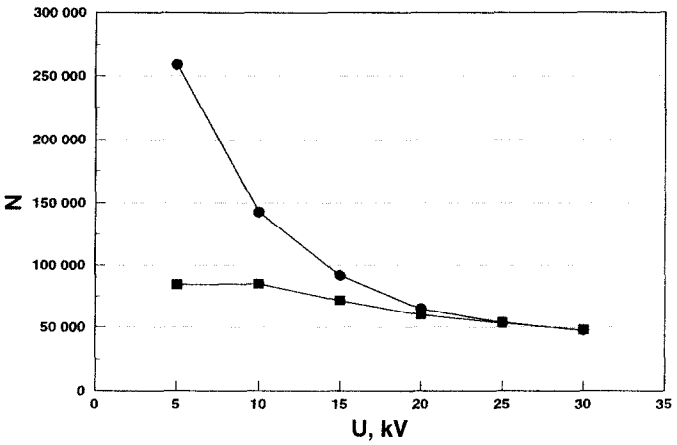

Fig. 1. Experimentally obtained number of theoretical plates (N) *vs.* the applied potential (U, kV) in experimental series 1. The 10 mM tricine running buffer (pH 8.0) contained 25 mM NaCl ($\kappa_{21^\circ C}$ = 2.75 mS cm^{-1}). B-hGH was either diluted with the running buffer [(■) (non-stacking, $\kappa_{21^\circ C}$ = 2.75 mS cm^{-1})] or distilled water [(●) (stacking, $\kappa_{21^\circ C}$ = 0.17 mS cm^{-1}). Sample was introduced for 3.0 s. The total length of the 50 μm I.D. capillary was L_c = 100 cm and the effective length was L_d = 75 cm. The other experimental conditions are given under Experimental. Changing from non-stacking to stacking conditions at low applied potentials greatly improved peak efficiencies.

Eqn. 1 is an easy-to-measure approximation of N applied to experimental data for Gaussian-shaped peaks. N is defined as

$$N = \frac{L_d^2}{\sigma^2} \tag{2}$$

where L_d is the effective length of the capillary and σ^2 is the total analyte zone variance. In the mathematical model we ascribe σ^2 to six terms: axial (σ^2_{axial}) and radial diffusion (σ^2_{radial}), a corrected length of the introduced analyte zone (σ^2_{intro}), detector length (σ^2_{det}), chromatographic effects (σ^2_{chrom}) and sample overload ($\sigma^2_{overload}$):

$$\sigma^2 = \sigma^2_{axial} + \sigma^2_{radial} + \sigma^2_{intro} + \sigma^2_{det} + \sigma^2_{chrom} + \sigma^2_{overload} \tag{3}$$

All six terms are functions of temperature, which has been accounted for in the dispersion model.

With the actual experimental conditions three of the terms were neglected:

$$\sigma^2_{overload} \approx 0 \tag{4}$$

$$\sigma^2_{chrom} \approx 0 \tag{5}$$

(as B-hGH is repelled from the silica surface at pH 8.0) and

$$\sigma^2_{det} = \frac{L^2_{det}}{12} \approx 0 \tag{6}$$

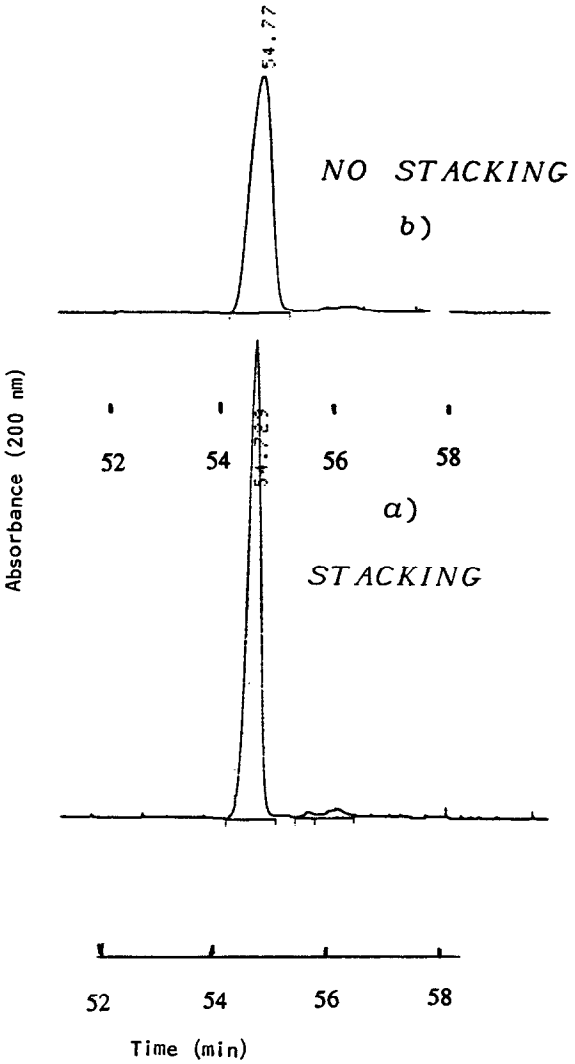

Fig. 2. Experimentally obtained 5-kV electropherograms of the series 1 (a) stacking and (b) non-stacking runs. The abscissa scaling is in minutes. In the stacking run N was *ca.* three times higher than that in the non-stacking run. The improved peak efficiency under stacking conditions is clearly demonstrated.

where L_{det} is the detector length (σ^2_{det} was, however, calculated for all the runs; in general it contributed no more than 1% to the total variance).

Axial dispersion after an eventual stacking process is calculated by the Einstein equation [18]:

$$\sigma^2_{axial} = 2D_B(t_R - t_0) \tag{7}$$

where D_B is the analyte diffusion coefficient when surrounded by running buffer and t_0 is the duration of an eventual stacking process, which we estimate by

$$t_0 = \frac{L_0}{\mu_{EP,S} E_S} \tag{8}$$

$\mu_{EP,S}$ and E_S being the electrophoretic analyte mobility in the sample zone and the field strength along the sample zone, respectively, and L_0 the analyte zone length immediately after sample introduction. Owing to a low ratio of introduction time to hGH diffusional time constant, it can be shown that the concentration profile is elongated into a triangular shape owing to the parabolic velocity profile during introduction [33]. Hence, in order to describe the analyte zone as a rectangular plug in the model, L_0 was multiplied by a factor of 2 (typical t_0 values were in the range 0.5–60 s).

Radial dispersion after an eventual stacking process is calculated as [33,34]

$$\sigma^2_{radial} = \frac{R^2_{inner} v^2}{2D_B} < wh > (t_R - t_0)\left[1 + k_R\left(\frac{\Delta v_{EO} L_0}{v L_c}\right)^2\right] \tag{9}$$

where v is the analyte zone velocity, R_{inner} is the capillary inner radius, k_R is a constant and L_c is the total capillary length. Under non-stacking conditions $1/<wh>$ is a function of the flow profile and the ionic strength ($1/<wh> = 12$ for laminar flow; in FSCE typical values are 1500–4000). Under stacking conditions $1/<wh>$ is a function of the difference between the sample solution and running buffer ionic strength (typical values are 200–1500 during stacking and 1500–6000 after the stacking period). An expression for $<wh>$ during the stacking process is derived in the Appendix. Δv_{EO} is the difference between the two electroosmotic flows that would be measured if the capillary had been filled only with sample solution or running buffer.

The variance due to the introduced analyte zone length is calculated as [30]

$$\sigma^2_{intro} = \frac{L_I^2}{12} \tag{10}$$

where L_I is the analyte zone length corrected for extraneous injection, for diffusional effects during introduction and for an eventual stacking process. Hence, only under non-stacking conditions does $L_0 = L_I$. Obviously, most attention has been drawn towards this term in the mathematical modelling.

Simulation of sampling stacking

Sample stacking is simulated as shown in Fig. 3a and b. The leading edge of the analyte zone migrates with a linear velocity equal to the velocity that would be measured if no stacking took place (sample buffer = running buffer). The terminating edge accounts for the zone stacking as it migrates faster than the leading edge.

The mole flux, j, through the capillary cross-sectional area is calculated relative to the "leading edge velocity":

$$j = C_S \mu_{EP,S} \Delta E \tag{11}$$

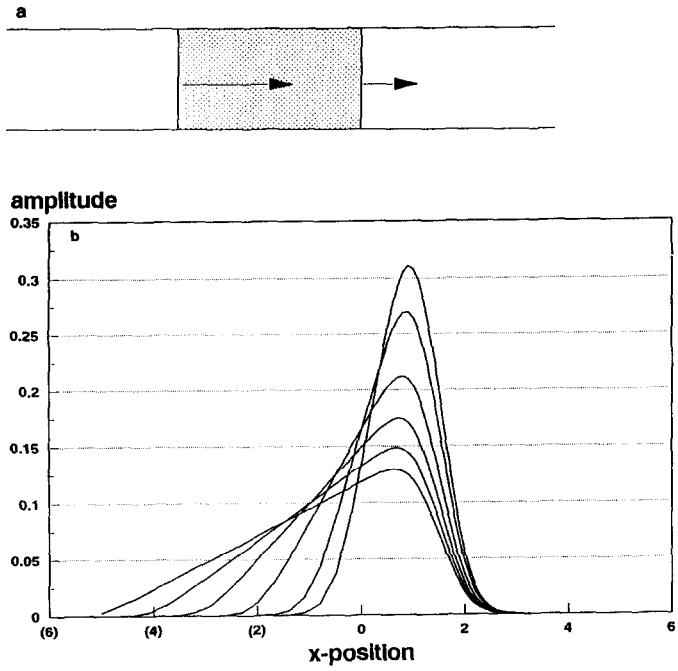

Fig. 3. Computer simulation of sample stacking. (a) One-dimensional; (b) two-dimensional. In the mathematical model it is assumed that the terminating edge of the analyte zone migrates faster than the leading edge, thus reducing the zone length. In (a) this is illustrated by the length of the arrows. In (b) axial position and amplitude are chosen arbitrarily.

where C_S is the analyte concentration in the sample zone. ΔE, which is the "stacking force", is the difference between the field strengths along the sample zone, E_S, and running buffer, E_B:

$$\Delta E = E_S - E_B = \frac{I}{A}\left(\frac{1}{\kappa_S} - \frac{1}{\kappa_B}\right) = \frac{U}{L_S + \frac{\kappa_S}{\kappa_B - \kappa_S} \cdot L_c} \tag{12}$$

where I, A, κ_S, κ_B, L_S and U are the current, the capillary cross-sectional area, the specific conductivities of the sample zone and running buffer, the analyte zone length (which varies during the stacking process) and the applied voltage, respectively.

It is assumed that the total amount of analyte is conserved in the sample zone during the stacking period:

$$C_S L_S = C_0 L_0 \tag{13}$$

where C_S is the analyte concentration when the zone length is L_S and C_0 is the analyte concentration immediately after the sample has been introduced with a corrected plug

length equal to L_0. Dividing eqn. 11 by C_S, combining with eqns. 12 and 13 and introducing the dimensionless length, y,

$$y \equiv \frac{L_S}{L_d} \tag{14}$$

yields

$$\frac{dy}{dt} = -\frac{\mu_{EP,S}U\left(\frac{\kappa_B}{\kappa_S} - 1\right)}{\left[\left(\frac{\kappa_B}{\kappa_S} - 1\right)L_S + L_c\right]L_d} = -\frac{1}{\tau_E}\left(\frac{\kappa_B}{\kappa_S} - 1\right) = -\frac{1}{\tau_B} \tag{15}$$

where τ_E and τ_B have the dimension time. During the stacking period axial and radial diffusion widen the analyte zone with increasing time, while the stacking force as expressed by eqn. 15 has a zone sharpening effect:

$$\frac{d(y^2)}{dt} = \text{axial diffusion} + \text{radial diffusion} - \text{stacking}$$

$$= 2\left(\frac{D_S}{L_d^2} + \frac{R_{inner}^2 \Delta v_{EO}^2 < wh >}{4D_S L_d^2}\right) - 2 \cdot \frac{y}{\tau_B} = 2\left(\frac{1}{\tau_A} - \frac{y}{\tau_B}\right) \tag{16}$$

D_S, which is the analyte diffusion coefficient when surrounded by the sample solution, is calculated as [35]

$$D_S = \frac{\mu_{EP,S}R_{gas}T}{z_{hGH}F} \tag{17}$$

where F is the Faraday constant (96 485 C mol^{-1}), R_{gas} is the gas constant (8.314 J K^{-1} mol^{-1}) and z_{hGH} is the net charge of the hGH molecule (calculated to be *ca.* -7).

If the sample plug was not sandwiched between the running buffer zones, the electroosmotic velocity would be higher in the sample zone compared with the corresponding velocity of the running buffer owing to a higher electroosmotic mobility (higher sample zone zeta potential, wider double layer) and a higher field strength (lower sample zone specific conductivity). The difference between the two velocities is the Δv_{EO} term in eqns. 9 and 16:

$$\Delta v_{EO} = \mu_{EO,S}E_S - \mu_{EO,B}E_B = \left(\mu_{EO,S} \cdot \frac{\kappa_B}{\kappa_S} - \mu_{EO,B}\right)E_B$$

$$= \left(\mu_{EO,S} \cdot \frac{\kappa_B}{\kappa_S} - \mu_{EO,B}\right)\frac{U}{\left(\frac{\kappa_B}{\kappa_S} - 1\right)L_0 + L_c} \tag{18}$$

The tendency for the sample zone to speed up the electroosmotic velocity results in an "electroosmotic pump" pressure on the running buffer. The motive force is in the loosely held part of the double layer close to the capillary wall. Hence, the Δv_{EO} velocity results in an additional dispersive force where the "electroosmotic pump" pressure from the sample zone must be balanced by a backflow.

The so-called electroosmotic flow profile is in general expressed by

$$\frac{v_{EO,S}}{v_{max,EO,S}} = 1 - R^n \tag{19}$$

where $v_{max,EO,S}$ is the maximum electroosmotic velocity of the sample zone (experienced at the tube axis) if the capillary was filled only with sample solution and R is the variable normed inner radius of the capillary tube. The higher the exponent value, n, the more plug-like is the profile. For laminar flow $n = 2$. Martin and co-workers [36,37] proposed the exponent to be 8.54 for electroosmotic flow.

Owing to the backflow we assume the flow profile during stacking conditions to be expressed as

$$\frac{v_{EO,S}}{v_{max,EO,S}} = [(1 - R^S) - k_S(1 - R^B)][1 + f(dT_{inner,S}, dT_{inner,B}, R)]$$

$$\approx (1 - R^S) - k_S(1 - R^B) \tag{20}$$

where k_S indicates the degree of backflow. $f(dT_{inner,S}, dT_{inner,B}, R)$ is a function of R and the sample zone and running buffer temperature elevations in the capillary tube. This function accounts for additional dispersion caused by Joule heating. Under the present experimental conditions it could be neglected [22]. An expression similar to eqn. 20 is derived for the running buffer flow profile.

S and B in eqn. 20 are the exponent n values for the sample zone and running buffer, respectively. They are assumed to be inversely proportional to the Debye layer [35] thickness, δ. Hence,

$$B = k_{DL} \cdot \frac{R_{inner}}{\delta_B} = k_{DL} R_{inner} \sqrt{\frac{F^2 \sum_{B,i} c_i z_i^2}{\varepsilon_0 \varepsilon_r R_{gas} T_B}} \tag{21}$$

$$S = k_{DL} \cdot \frac{R_{inner}}{\delta_S} = k_{DL} R_{inner} \sqrt{\frac{F^2 \sum_{S,i} c_i z_i^2}{\varepsilon_0 \varepsilon_r R_{gas} T_S}} \tag{22}$$

where k_{DL} is a proportionality constant (experimental data fit, $k_{DL} = 0.025$), ε_0 is the permittivity of vacuum ($8.854 \cdot 10^{-14}$ C^2 cm^{-1} J^{-1}), ε_r is the relative permittivity, T_S and T_B are the temperatures of the sample zone and running buffer, respectively, and c_i and z_i are the concentration of and the net number of elementary charges on the ith electrolyte, respectively.

Calculation of k_S in eqn. 20 is based on the demands of a constant mass flow, which means that the difference between the buffer and sample zone mean velocities must equal zero:

$$2\int_{R=0}^{R=1}\left(v_{EO,S} - v_{EO,B}\right)RdR = 0$$

$$\Leftrightarrow$$

$$2\int_{R=0}^{R=1}\{v_{max,EO,S}[1 - R^S - k_S(1 - R^B)] - v_{max,EO,B}[1 - R^B + k_B(1 - R^S)]\}\,RdR = 0 \quad (23)$$

As the electroosmotic pump pressure on the buffer zone is balanced by a back-pressure on the sample zone, k_B can be expressed in terms of k_S:

$$k_B = k_S \cdot \frac{L_0\eta_S}{(L_c - L_0)\eta_B} \quad (24)$$

where η is the viscosity. Eqn. 24 is inserted in eqn. 23, which is solved for k_S:

$$k_S \approx \frac{\Delta v_{EO}}{v_{max,EO,S}} = 1 - \frac{v_{max,EO,B}}{v_{max,EO,S}} \quad (25)$$

In this solution it is assumed that $B \gg 1$, $S \gg 1$ and $L_c \gg L_0$. The equation expresses that the extent of backflow is proportional to Δv_{EO}.

Fig. 4a and b are computer simulations illustrating sample zone profiles as expressed by eqn. 20 during stacking conditions for various $v_{max,EO,S}/v_{max,EO,B}$ values in the range 1–10 (corresponding to the k_S range 0.0–0.9). $v_{max,EO,B}$ was set equal to 1.

At the tube axis the flow profile remains plug-like, but close to the capillary wall the difference between the electroosmotic force in the running buffer and sample zone double layers results in more laminar-like profiles. Very close to the wall the backflow is even stronger than the forward flow resulting in a net negative flow.

As all the parameters in the differential eqn. 16 are now accounted for, it can be solved. Integration from y_0 to y yields

$$\frac{ay_0}{1 - \frac{\tau_E}{\tau_S}} - ay + \ln\left(\frac{ay_0 - 1}{ay - 1}\right) = 0, \qquad a = \frac{\tau_A}{\tau_B} \quad (26a)$$

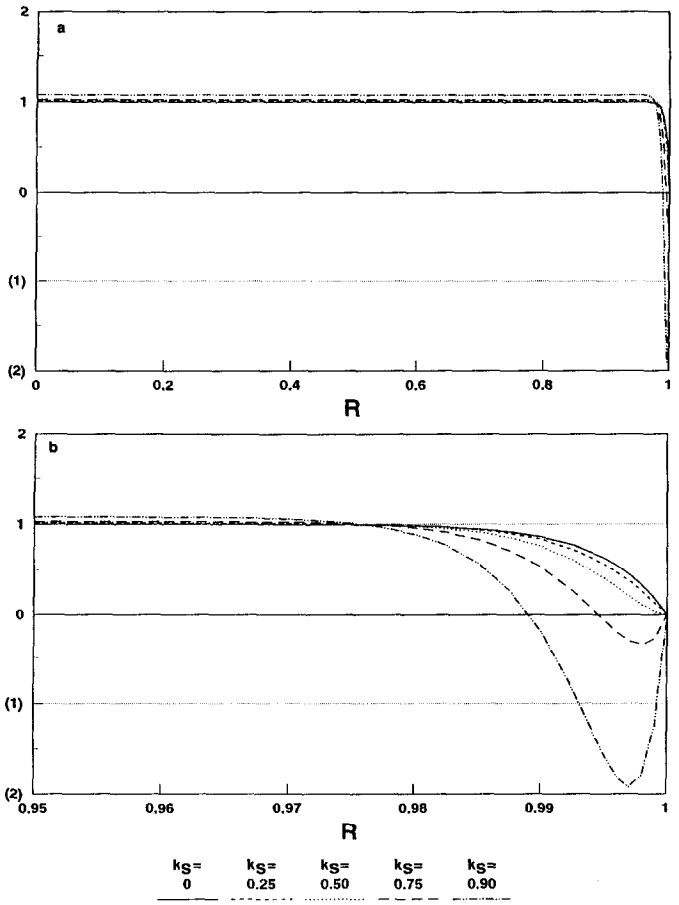

Fig. 4. Computer simulation of the electroosmotic flow profile ($v_{EO,S}$) as a function of the variable normed radial position, R, in the capillary during stacking conditions as calculated by eqn. 20. (a) $0 < R < 1$; (b) $0.95 < R < 1$. The profile is shown for different k_S values in the range 0–0.9. The $v_{max,EO,B}$ value was chosen arbitrarily to be 1.00. Owing to the lower double layer thickness in the running buffer relative to the sample zone, there is a net negative flow very close to the wall. The higher the k_S value (eqn. 25) the more laminar-like is the profile and thereby the larger is the dispersion.

or, expressed by the specific conductivities of the sample zone, κ_S, and running buffer, κ_B:

$$\frac{\kappa_S}{\kappa_B} \cdot ay_0 - ay + \ln\left(\frac{ay_0 - 1}{ay - 1}\right) = 0, \qquad a = \frac{\tau_A}{\tau_B} \tag{26b}$$

Eqn. 26a or 26b is solved iteratively with respect to y.

The ratio of the originally introduced sample zone length to the analyte zone length after the stacking period, $L_0/L_1 = y_0/y$, is a measure of the sample stacking.

Retention time per theoretical plate, t_R/N

Eqns. 7, 9 and 10 represent the contribution of each of the three variance terms (σ^2_{axial}, σ^2_{radial} and σ^2_{intro}) to the total variance (σ^2, cm^2). In the discussion below, the three terms are expressed as contributions to the total retention time per theoretical plate, t_R/N. Hence,

$$\frac{t_R}{N} = \frac{t_R}{L_d^2} \cdot \sigma^2$$

$$= \frac{t_R}{L_d^2}(\sigma^2_{axial} + \sigma^2_{radial} + \sigma^2_{intro})$$

$$= \chi_{axial} + \chi_{radial} + \chi_{intro} = \text{"axial"} + \text{"radial"} + \text{"intro"} \quad (27)$$

In this way the dispersive terms are calculated as

$$\text{"axial"} = \chi_{axial} = 2 \cdot \frac{D_B}{L_d^2} \cdot t_R^2 \left(1 - \frac{t_0}{t_R}\right) \quad (28)$$

$$\text{"radial"} = \chi_{radial} = \frac{R^2_{inner}}{2D_B} < wh > \left(1 - \frac{t_0}{t_R}\right)\left[1 + k_R\left(\frac{\Delta v_{EO} L_0}{v L_c}\right)^2\right] \quad (29)$$

$$\text{"intro"} = \chi_{intro} = \frac{t_R}{12} \cdot y^2 \quad (30)$$

As t_R/N denotes the retention time required to obtain one theoretical plate, the lower the t_R/N value the higher is the peak efficiency at any given t_R value.

RESULTS AND DISCUSSION

The ratio of the originally introduced sample zone length to the analyte zone length after the stacking period, $y_0/y = L_0/L_I$, expresses the sample stacking. For each run the experimentally measured and calculated values are inserted in eqn. 26. The equation is solved iteratively with respect to y. The estimated y_0/y ratios are depicted *vs.* U (Fig. 5) and ay_0 (Fig. 6) for the stacking and non-stacking runs in series 1. The dotted lines in Fig. 6 indicate the solution of eqn. 26 for various theoretical κ_B/κ_S values (given in the caption). The higher the ordinate value the more the analyte zone is reduced in length during the stacking process.

Running under stacking conditions has a dramatic effect on the analyte zone length. Reductions of nearly ten times are obtained for low applied voltages. At higher voltages the dispersive effects caused by the Δv_{EO} and $< wh >$ terms of the radial dispersion during the stacking period (eqn. 16) and the decreasing κ_B/κ_S ratio due to the temperature effects [22] (observed in Fig. 6) become more dominant.

The effect of different stacking powers (defined as ΔE, experimental series 2) is shown in Fig. 7. When there is only a low stacking power the analyte zone is stacked by a factor of *ca.* κ_B/κ_S (the 0 m*M* NaCl running buffer runs, $\kappa_B/\kappa_S \approx 1.3$).

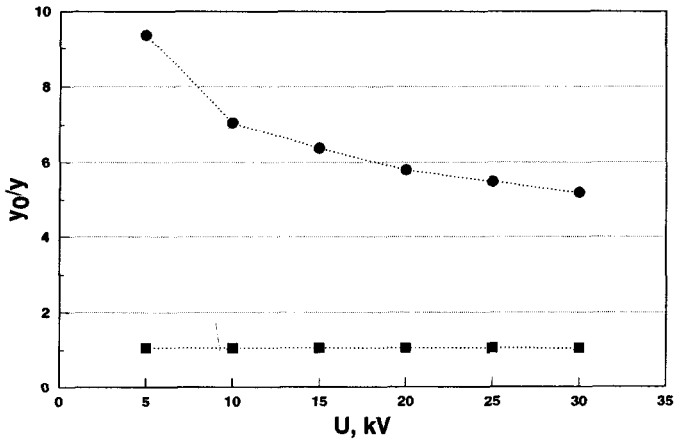

Fig. 5. Mathematical model, $y_0/y = L_0/L_1$ values *vs.* the applied potential (U, kV) in the series 1 experiment. During the stacking process (●) the original introduced analyte zone is reduced in length ($y_0/y > 1$), whereas in the non-stacking runs (■) the zone length is not reduced.

The 50 m*M* NaCl running buffer runs (Fig. 7) show an example of the increased radial dispersion nearly outbalancing the zone narrowing stacking effect due to the "backflow profile". Hence the analyte zone width is reduced more effectively in the 25 m*M* NaCl running buffer runs at high applied potentials compared with the 50 m*M* NaCl running buffer runs even though the specific conductivity ratio of the running buffer to sample zone is larger in the latter.

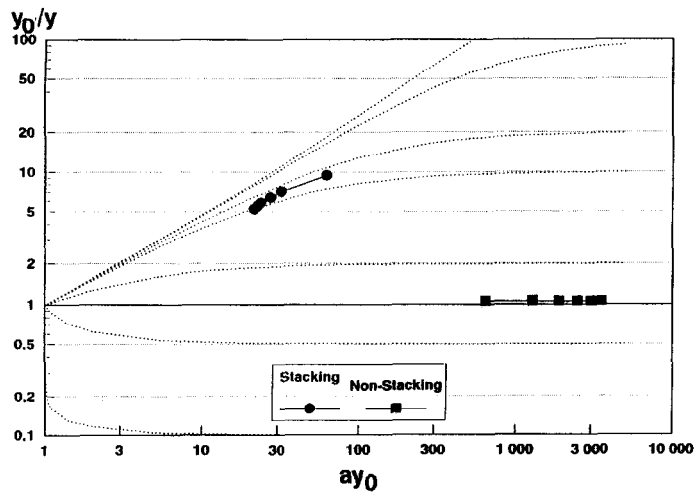

Fig. 6. Mathematical model, $y_0/y = L_0/L_1$ values *vs.* ay_0 in the series 1 experiment. The dotted lines indicate the solution of eqn. 26 for various κ_B/κ_S values. The values from top to bottom are 1000, 100, 20, 10, 2, 1 (horizontal solid line), 0.5 and 0.1. In the stacking runs (●) ay_0 increases with decreasing U. Hence, the figure illustrates that the κ_B/κ_S ratio decreases with increasing U caused by temperature effects [22]. (■) Non-stacking.

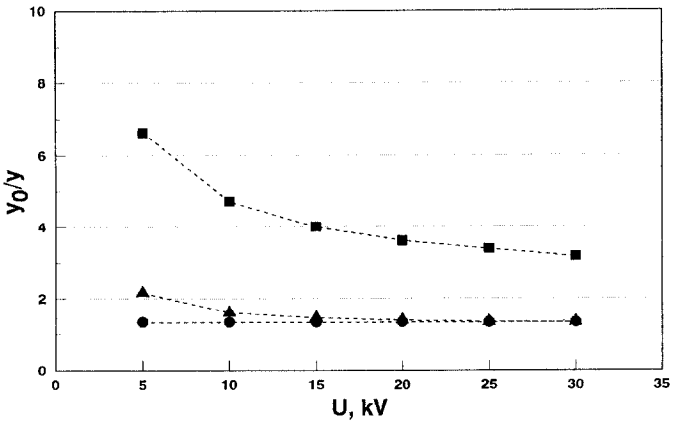

Fig. 7. Mathematical model, $y_0/y = L_0/L_1$ values *vs.* the applied potential (U, kV) in the series 2 experiment. During the stacking process the originally introduced analyte zone is reduced in length ($y_0/y > 1$). Increasing the κ_B/κ_S ratio (increasing NaCl concentration) increases the stacking power (ΔE), but at the same time radial dispersion increases. NaCl concentration: ● = 0; ■ = 25; ▲ = 50 mM.

Comparing mathematical model and experimental results

Series 1, stacking vs. non-stacking. Fig. 8 shows the correlation between the mathematical dispersion model (dashed lines) and the experimentally obtained results (solid lines) in series 1, where the purpose was to show the effect of stacking on peak efficiency. The lower the t_R/N value the higher is the peak efficiency at any given t_R value.

At high applied potentials (20–30 kV), similar and almost constant t_R/N values are obtained for the stacking and non-stacking runs. When U is lowered t_R/N increases

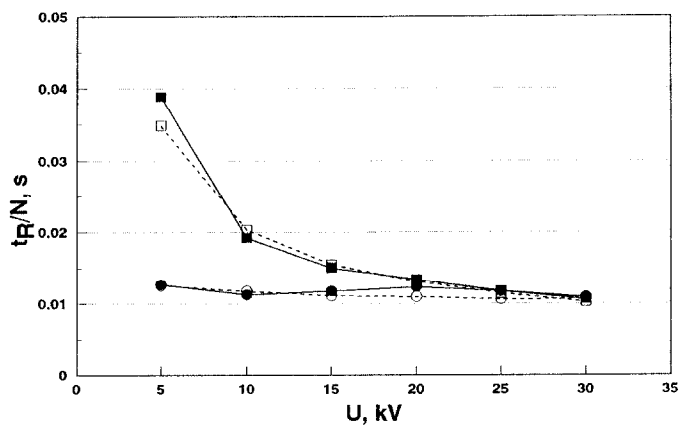

Fig. 8. t_R/N (s) *vs.* the applied potential (U, kV) in the series 1 experiment. The solid lines are experimental curves based on eqn. 1 and the dashed lines are based on the mathematical model (eqn. 27). At low applied potentials, turning from non-stacking (■, □) to stacking conditions (●, ○) greatly improves peak efficiency (decreasing t_R/N). Similar retention times were obtained in the stacking and non-stacking runs at each applied potential.

when the runs are carried out under non-stacking conditions, whereas the value remains almost constant for the stacking runs. The reason for this difference between the non-stacking and stacking runs is revealed by comparing Fig. 9a (stacking) and b (non-stacking), where each of the three additive dispersion terms in eqn. 27 of the mathematical model are plotted. Owing to the narrowed analyte zone length during stacking, the introduction term is much lower in the stacking runs than the non-stacking runs, where it is the largest dispersive contributor at low applied voltages (5–15 kV) owing to its "proportionality" to the analysis time (eqn. 30).

In the non-stacking runs the radial dispersion is lower than in the stacking runs as the $\Delta v_{EO}/v$ term in eqn. 29 is negligible.

Fig. 10 depicts the relative contribution of each of the three additive dispersion terms in each of the runs in stacked-bar form. Radial dispersion is the dominant zone broadener during the stacking runs, contributing 88–98% of the total dispersion.

Axial diffusion is an important quantitative term only when there is a long analysis time, and hence at low applied voltages. One of the explanations for the difference between the experimental and theoretical t_R/N values in the 5-kV runs (Fig. 8) is that the axial dispersion values in general may be estimated too low in the model.

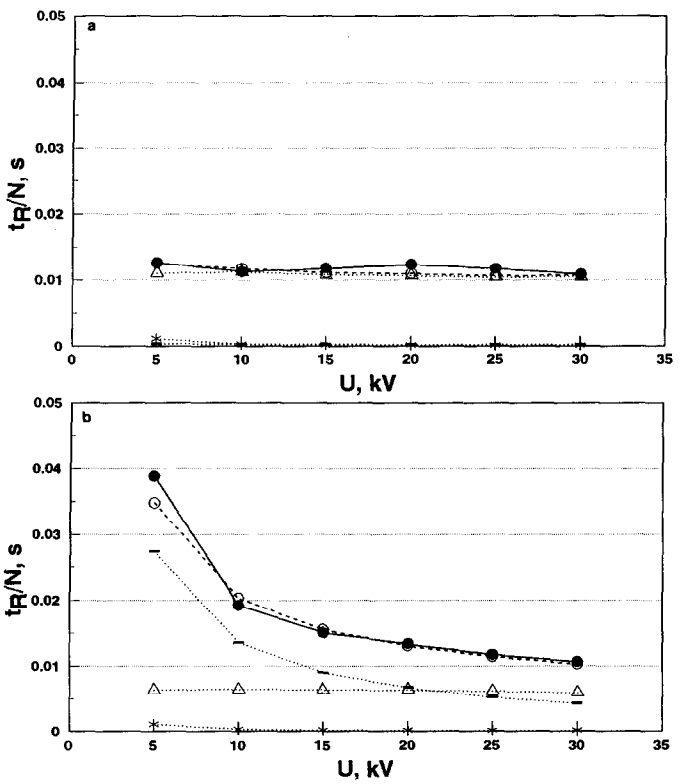

Fig. 9. t_R/N (s) *vs.* the applied potential (U, kV) in the series 1 experiment when (a) stacking or (b) non-stacking conditions were used. The mathematical model values for each of the three additive dispersive terms in eqn. 27 are shown. ● = Experimental. Models: ○ = total; ✳ = axial; △ = radial; — = introduction.

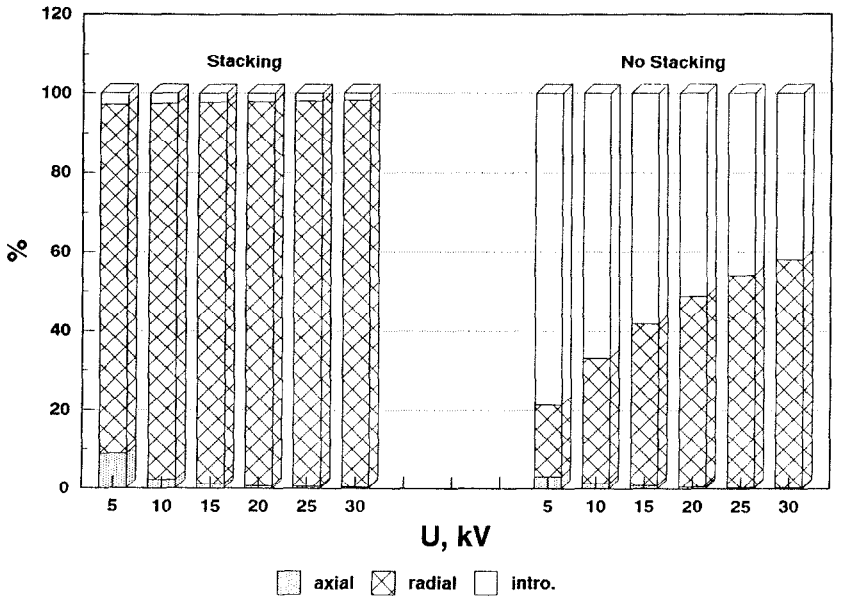

Fig. 10. Experimental series 1. Each of the three dispersive terms in eqn. 27 as a percentage of the total dispersion during analysis is shown in stacked bar form for each of the runs. Left side, stacking; right side, non-stacking. During the stacking runs the introduction term percentage value is much lower than in the corresponding non-stacking runs.

The results of the series 1 experiment suggest a low potential to be applied under stacking conditions as the t_R/N value is almost constant with varying U in the range 5–30 kV. Hence, the longer the analysis time, the higher is the number of theoretical plates is obtained. At very low voltages (5 kV and below) axial diffusion does, however, increase t_R/N, thus creating a lower limit to the applied potential.

Fig. 1 shows the theoretical plate numbers vs. U in the series 1 experiment. McCormick [9] reported similar observations, with low applied voltages giving the highest number of theoretical plates. Separation was improved when the operating voltage was applied as a gradient instead of instantly. McCormick [9] did not discuss the reasons for these observations, but according to the present model the latter phenomenon might be due to a lower radial dispersion when applying the voltage as a gradient.

Prestacking is used to describe the use of low U values during the initial stacking period, t_0, followed by a higher U when the analyte zone has left the original introduced sample plug. Prestacking has proved very useful in our laboratory, serving the purpose of reducing retention times yet giving high peak efficiencies.

Series 2, different stacking powers (ΔE). Fig. 11 shows the correlation between the mathematical dispersion model (dotted lines) and the experimental results (solid lines) in series 2, where the purpose was to show the effect of stacking power, ΔE, on peak efficiency.

The lowest t_R/N values are obtained when there is only a low stacking power (0 mM NaCl running buffer), and hence a low κ_B/κ_S value above unity. Fig. 12a (0 mM

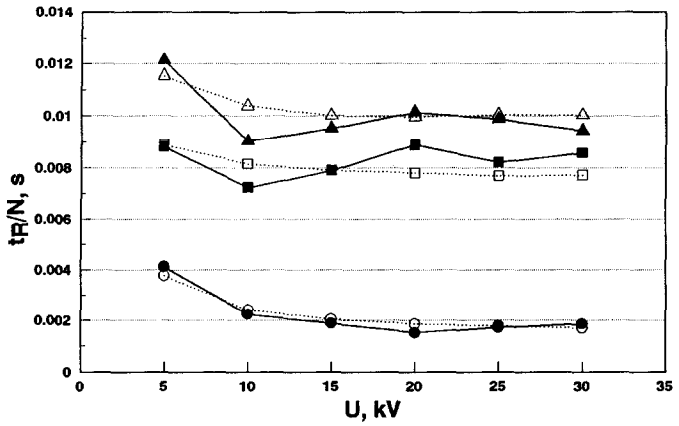

Fig. 11. t_R/N (s) *vs.* the applied potential (U, kV) in the series 2 experiment. The solid lines are experimental curves based on eqn. 1 and the dotted lines are based on the mathematical model (eqn. 27). At each applied potential the retention time order was 50 mM NaCl (▲,△) > 25 mM NaCl (■,□) > 0 mM NaCl (●,○).

NaCl), b (25 mM NaCl) and c (50 mM NaCl), which show each of the three additive dispersive terms of eqn. 27, elaborate this. Increasing the initial κ_B/κ_S value above unity at any given U results in a higher stacking power, thus increasing the narrowing of the original analyte zone length. At the same time, however, radial dispersion increases, thus opposing the narrowing effect of the stacking power.

Increasing the applied potential (and thereby ΔE) has the same general effect: stacking the analyte zone, but at the same time increasing the radial dispersion.

As in the series 1 experiment, it is only at low applied potentials (long analysis time) that the axial term has any quantitative importance with respect to the total dispersion (Fig. 13).

The series 2 experiment is substantial in the discussion of dispersion during FSCE analysis with stacking conditions. Moring *et al.* [38] discussed the importance of sample stacking during FSCE analysis and argued that "much lower ionic strength and conductivity" of the sample solution relative to the running buffer (thus high κ_B/κ_S ratios) should be employed, resulting in very narrow analyte zones. The experimental results as illustrated in Figs. 11 and 14 (N *vs.* U, experimental series 2) oppose this suggestion. Whereas it takes *ca.* 2 ms to obtain one theoretical plate in the 20 kV, 0 mM NaCl run, it takes *ca.* 9 and 10 ms in the 20 kV, 25 mM and 50 mM NaCl runs where the κ_B/κ_S values are higher.

Hence, increasing the κ_B/κ_S ratio has a narrowing effect on the analyte zone, as discussed by Moring *et al.* [38], but at the same time the radial dispersion both during and after the stacking period increases, as observed in Fig. 12a–c where the radial term increases from the 0 to the 25 to the 50 mM NaCl runs.

As in series 1, radial dispersion is the main zone broadener at high applied potentials (Fig. 13) and at high κ_B/κ_S ratios.

An additional experimental series was carried out. Different plug lengths were introduced (0.2–15-s introduction) and the experiments were performed under stacking, no stacking or reversed stacking conditions ($\kappa_B < \kappa_S$) in 10 mM tricine buffer (pH 8.0).

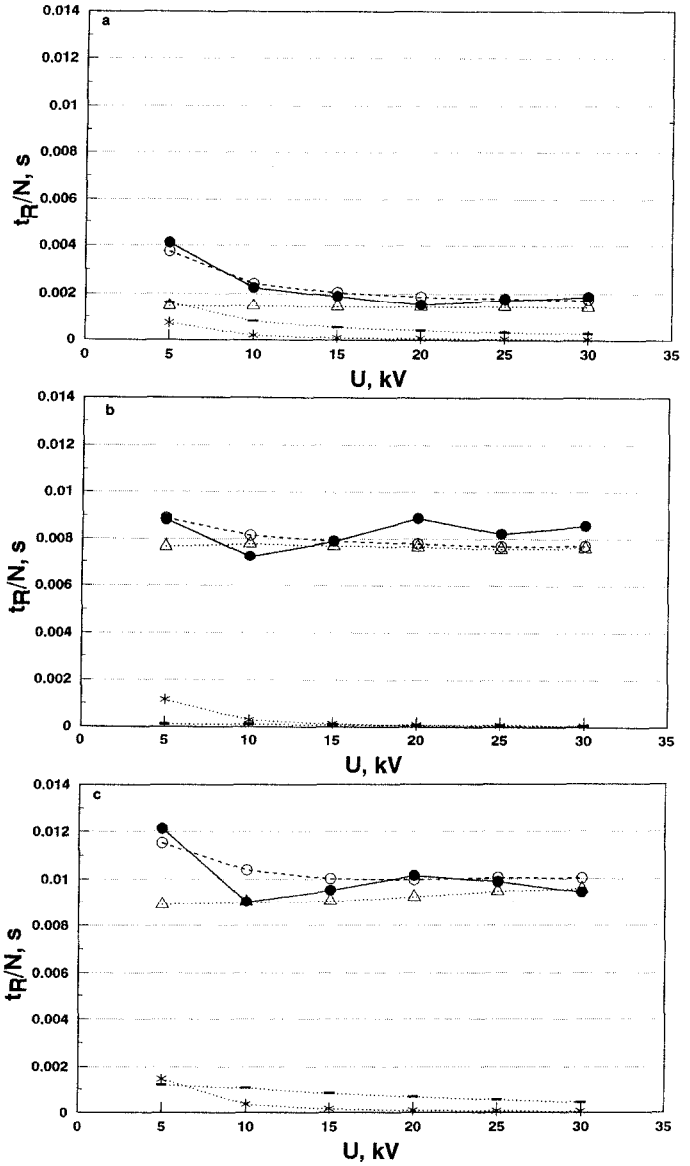

Fig. 12. t_R/N (s) *vs.* the applied potential (U, kV) in the series 2 experiment when the 10 mM tricine running buffer (pH 8.0) contained (a) 0, (b) 25 or (c) 50 mM NaCl. The values for each of the three dispersive terms in eqn. 27 are shown. Increasing the κ_B/κ_S ratio (increasing the NaCl concentration in the running buffer) strongly increases radial dispersion and the t_R/N values. Symbols as in Fig. 9.

Increasing the introduction time, t_{inj}, dramatically decreased the peak efficiency (Fig. 15) as the introduction term of the total dispersion becomes more dominant with longer injection times [30] (eqn. 30). In the 0.2-s non-stacking run the introduction term contributed *ca.* 1% to the total dispersion whereas for a 15-s introduction the

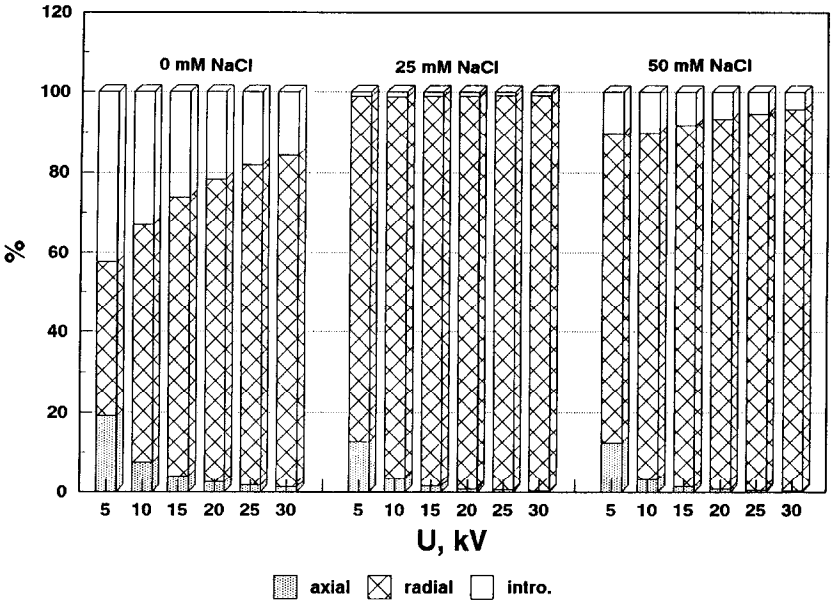

Fig. 13. Experimental series 2. Each of the three dispersive terms in eqn. 27 as a percentage of the total dispersion during analysis is shown in stacked bar form for each of the runs. Left side, 0 m*M* NaCl; middle, 25 m*M* NaCl; right side, 50 m*M* NaCl. Only at low applied potentials and with low stacking power (0 m*M* NaCl) does the introduction term exceeds 20% of the total dispersion.

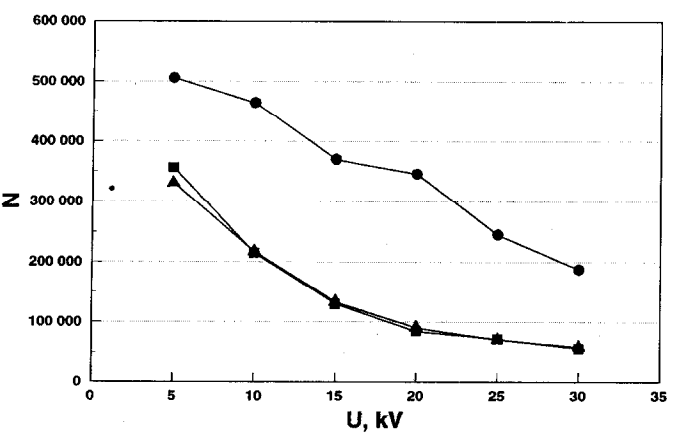

Fig. 14. Number of experimentally obtained theoretical plates (*N*) *vs.* the applied potential (*U*, kV) in the series 2 experiment. The t_R/N values are higher in the 50 m*M* NaCl runs than in the 25 m*M* NaCl runs at each applied potential. As the retention time is longer in the 50 m*M* runs, however, with this combination of t_R/N and t_R almost identical *N* values were obtained in the two buffers. NaCl concentration: (●) 0; (■) 25; (▲) 50 m*M*.

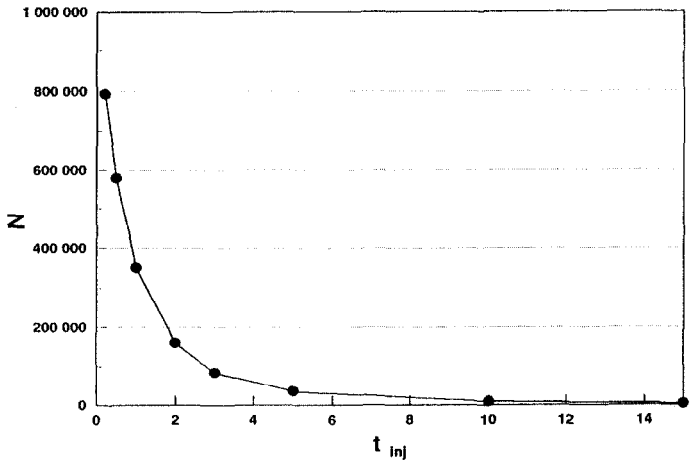

Fig. 15. Number of experimentally obtained theoretical plates (N) *vs.* the introduction time (t_{inj}, s). Increasing t_{inj} dramatically decreases N. Experimental conditions: sample, B-hGH diluted to 0.1 mg ml^{-1} with distilled water ($\kappa_{21°C}$ = 0.17 mS cm^{-1}); running buffer, 10 mM tricine (pH 8.0) ($\kappa_{21°C}$ = 0.22 mS cm^{-1}); samples introduced for 0.2–15 s; applied potential, 15 kV. Other conditions as under Experimental.

value was *ca.* 98%. Hence, with long sample introduction times, where the introduction dispersion term is totally dominant, a stacking process can be very effective in narrowing the analyte zone length. Changing from stacking to non-stacking conditions decreased t_R/N by a factor of 5–10 in the t_{inj} = 15 s runs.

In the reversed stacking runs the original analyte zone was widened relative to the originally introduced sample plug length. If experiments have to be carried out under reversed stacking conditions, short injection times should be used.

CONCLUSIONS

Based on simple assumptions in the development of the mathematical model for dispersion during FSCE analysis, a few general suggestions can be made.

Stacking is a powerful technique in narrowing the analyte zone length, thus increasing the number of theoretical plates.

The specific conductivity of the running buffer should be kept low in order to avoid dispersive effects caused by excessive Joule heating.

Stacking conditions ($\kappa_S/\kappa_B < 1$) should be employed and the specific conductivity of the sample solution should only be slightly lower than that of the buffer solution. We term this "moderate stacking".

Increasing the κ_B/κ_S ratio increases the stacking power (ΔE), reducing the analyte zone length, but at the same time the radial dispersion is increased, thus widening the analyte zone. With increasing κ_B/κ_S ratios and increasing applied potentials the radial dispersion dominates over the "zone stacking". Hence, the applied potential should be kept low during the stacking period, t_0, with a lower limit governed by axial diffusion.

After the stacking period the analyte zone has left the originally introduced sample zone and the applied potential can be increased in order to speed up analysis. It

must be kept in mind, however, that according to the model the originally introduced sample zone exerts an electroosmotic pump pressure on the analyte zone even after the stacking period, resulting in a radial dispersion which increases slightly with increasing potential.

If long introduction times are necessary owing to, *e.g.*, a low analyte concentration in the sample solution and/or a low detector sensitivity, moderate stacking conditions and low applied potentials are very effective in narrowing the analyte zone and superior to non-stacking and reversed stacking experimental conditions.

In accordance with existing FSCE theory, the mathematical model predicts that the number of theoretical plates increases with decreasing introduction time.

If reversed stacking conditions cannot be avoided, the introduction time should be kept as short as possible.

In summary, generally the introduction time should be medium to short depending on the detector performance, moderate stacking conditions and low applied potentials should be employed during the stacking period, the running buffer conductivity should be kept as low as possible and the applied potential should be increased after the stacking period (depending on the κ_B/κ_S and κ_B values) in order to speed up analysis.

APPENDIX

Calculation of $<wh>$ during stacking

The term w is a velocity profile function of the normed radius, R, and defined as [33]

$$w = m \cdot \frac{v_{EO,S}}{v_{max,EO,S}}$$

$$= m[1 - R^S - k_S(1 - R^B)]$$

$$= m[1 - z^n - k_S(1 - z^u)] \tag{A1}$$

$$n \equiv \frac{S}{2}; \qquad u \equiv \frac{B}{2}; \qquad z \equiv R^2$$

n, u and z are introduced in order to simplify the mathematical manipulations concerning the mean of the wh product ($= <wh>$).

Here m is a constant which meets the demand that the mean value of $w = 1$:

$$<w> \equiv 1 \tag{A2a}$$

$$\Leftrightarrow$$

$$\int_{z=0}^{z=1} m[1 - z^n - k_S(1 - z^u)]\,dz = 1 \tag{A2b}$$

$$\Leftrightarrow$$

$$m = \frac{1}{\frac{n}{n+1} - \frac{u}{u+1} \cdot k_S} \tag{A2c}$$

This means that eqn. A1 can be rewritten as

$$w = \frac{1 - z^n - k_S(1 - z^u)}{\frac{n}{n+1} - \frac{u}{u+1} \cdot k_S} \tag{A3}$$

In this equation h is a function of the radial position z and stationary solution to the concentration profile in the Taylor approximation [39] of the solution to the dispersed plug flow model [33,39,40]:

$$-\nabla^2 h = -\frac{\partial}{\partial z}\left(z \cdot \frac{\partial h}{\partial z}\right) = w - 1 \tag{A4}$$

The equation is solved by the use of eqn. A3 and the boundary conditions

$$<h> = 0, \qquad \frac{\partial h(1)}{\partial z} = 0$$

thus yielding

$$h = \frac{-\frac{1}{(n+1)} + \frac{1}{(n+1)^2} \cdot z^{n+1} + k_S \cdot \frac{1}{u+1} \cdot z - k_S \cdot \frac{1}{(u+1)^2} \cdot z^{u+1}}{\frac{n}{n+1} - k_S \cdot \frac{u}{u+1}} + h_0 \tag{A5}$$

After extensive calculations and reductions, the mean value of the product wh is found to be

$$<wh> = \frac{n^2}{2(n+1)^3(n+2)} \Bigg/ \left(\frac{n}{n+1} - k_S \cdot \frac{u}{u+1}\right)^2$$

$$- k_S \cdot \frac{un \cdot \frac{(n+4) + u(n+5) + u^2}{(n+1)(u+1)^2(n+2)(u+2)(n+u+2)}}{\left(\frac{n}{n+1} - k_S \cdot \frac{u}{u+1}\right)^2} + k_S^2 \cdot \frac{\frac{u^2}{2(u+1)^3(u+2)}}{\left(\frac{n}{n+1} - k_S \cdot \frac{u}{u+1}\right)^2} \tag{A6}$$

If there is no backflow (no stacking), $k_S = 0$ and eqn. A6 reduces to

$$<wh> = \frac{1}{2(n+1)(n+2)} \tag{A7}$$

For laminar flow where $n = S/2 = 1$, the value of $<wh>$ is 1/12, as used by, *e.g.*, Golay and Atwood [34]. The higher the value of n, the lower is the value of $<wh>$ and, in accordance with eqn. 16, the lower is the radial dispersion.

As generally $n \gg 1$ and $u \gg 1$, eqn. A6 is simplified to

$$<wh> \approx \frac{1}{2}\left(\frac{k_S - \frac{1}{u} - \frac{1}{n}}{1 - k_S}\right)^2 \tag{A8}$$

Inserting the expression for k_S as found in eqn. 25 into eqn. A8 yields

$$<wh> \approx \frac{1}{2k_{DL}^2}\left[\frac{v_{max,EO,S}}{v_{max,EO,B}}\left(\frac{\delta_B}{r} - \frac{\delta_S}{r}\right) - \frac{\delta_B}{r}\right]^2 \tag{A9}$$

In practice, the $<wh>$ values change as a function of time [33]. We did, however, simply calculate them as being constant in each separate run by the use of eqn. A9. The constant k_{DL} is estimated based on a trial-and-error best fit for all three experimental series and we chose a value of 0.025. The $<wh>$ term after the stacking process was chosen to fit the experimental data.

REFERENCES

1 B. L. Karger, A. S. Cohen and A. Guttman, *J. Chromatogr.*, 492 (1988) 585.
2 W. G. Kuhr, *Anal. Chem.*, 62 (1990) 403R.
3 H. Lüdi, E. Gassmann, H. Grossenbacher and W. Märki, *Anal. Chim. Acta*, 213 (1988) 215.
4 P. D. Grossman, J. C. Colburn, H. H. Lauer, R. G. Nielsen, R. M. Riggin, G. S. Sittampalam and E. C. Rickard, *Anal. Chem.*, 61 (1989) 1186.
5 J. Frenz, S.-L. Wu and W. S. Hancock, *J. Chromatogr.*, 480 (1989) 379.
6 R. G. Nielsen, R. M. Riggin and E. C. Rickard, *J. Chromatogr.*, 480 (1989) 393.
7 P. D. Grossman, J. C. Colburn and H. H. Lauer, *Anal. Biochem.*, 179 (1989) 28.
8 H. H. Lauer and D. McManigill, *Anal. Chem.*, 58 (1986) 166.
9 R. M. McCormick, *Anal. Chem.*, 60 (1988) 2322.
10 M. V. Novotny, K. A. Cobb and J. Liu, *Electrophoresis*, 11 (1990) 735.
11 A. Vinther, S. E. Bjørn, H. H. Sørensen and H. Søeberg, *J. Chromatogr.*, 516 (1990) 175.
12 A. Vinther, A. M. Jespersen, H. H. Sørensen and H. Søeberg, *Talanta*, (1991) in press.
13 M. M. Bushey and J. W. Jorgenson, *J. Chromatogr.*, 480 (1989) 301.
14 J. S. Green and J. W. Jorgenson, *J. Chromatogr.*, 478 (1989) 63.
15 S. Hjertén, *Electrophoresis*, 11 (1990) 665.
16 F. Foret, M. Deml and P. Bocek, *J. Chromatogr.*, 452 (1988) 601.
17 S. Terabe, K. Otsuka and T. Ando, *Anal. Chem.*, 61 (1989) 251.
18 J. W. Jorgenson and K. D. Lukacs, *Anal. Chem.*, 53 (1981) 1298.
19 J. W. Jorgenson and K. D. Lukacs, *Science*, 222 (1983) 266.
20 H. H. Lauer and D. McManigill, *Trends Anal. Chem.*, 5 (1986) 11.
21 J. W. Jorgenson, *New Directions in Electrophoretic Methods*, American Chemical Society, Washington, DC, 1987, Ch. 13, pp. 182–198.

22 A. Vinther and H. Søeberg, *J. Chromatogr.*, 559 (1991) 27.
23 E. Grushka, R. M. McCormick and J. J. Kirkland, *Anal. Chem.*, 61 (1989) 241.
24 A. E. Jones and E. Grushka, *J. Chromatogr.*, 466 (1989) 219.
25 J. H. Knox, *Chromatographia*, 26 (1988) 329.
26 J. H. Knox and K. A. McCormack, *J. Liq. Chromatogr.*, 12 (1989) 2435.
27 K. D. Lukacs and J. W. Jorgenson, *J. High Resolut. Chromatogr. Chromatogr. Commun.*, 8 (1985) 407.
28 W. Th. Kok, *Zone Broadening in Capillary Zone Electrophoresis*, Amsterdam Summer Course in Capillary Zone Electrophoresis, University of Amsterdam, Amsterdam, 1990.
29 E. Grushka and R. M. McCormick, *J. Chromatogr.*, 471 (1989) 421.
30 X. Huang, W. P. Coleman and R. N. Zare, *J. Chromatogr.*, 480 (1989) 95.
31 F. M. Everaerts, J. L. Beckers and Th. P. E. M. Verheggen, *Isotachophoresis —Theory, Instrumentation and Applications*, Elsevier, Amsterdam, 1976.
32 V. P. Burolla, S. L. Pentoney and R. N. Zare, *Am. Biotechnol. Lab.*, Nov./Dec. (1989) 7:10, 12.
33 H. Søeberg, *Course on Dispersion Models*, Department of Chemical Engineering, Technical University of Denmark, Lyngby, 1989.
34 M. J. E. Golay and J. G. Atwood, *J. Chromatogr.*, 186 (1979) 353.
35 P. W. Atkins, *Physical Chemistry*, Oxford University Press, Oxford, 1982.
36 M. Martin and G. Guiochon, *Anal. Chem.*, 56 (1984) 614.
37 M. Martin, G. Guiochon, Y. Walbroehl and J. W. Jorgenson, *Anal. Chem.*, 57 (1985) 559.
38 S. E. Moring, J. C. Colburn, P. D. Grossman and H. H. Lauer, *LC·GC Int.*, 3 (1989) 46.
39 G. Taylor, *Proc. R. Soc. London, Ser. A*, 219 (1953) 186.
40 O. Levenspiel, *Chemical Reaction Engineering*, Wiley, Toronto, 1972.